


Article

Screening and Investigation on Inhibition of Sediment Formation in a Kuwait Light Crude Oil by Commercial Additives with Some Guidelines for Field Applications

A. Qubian ¹, A. S. Abbas ¹, N. Al-Khedhair ¹, J. F. Peres ¹, D. Stratiev ^{2,3}, I. Shishkova ², R. Nikolova ⁴, V. Toteva ⁵ and M. R. Riazi ^{6,7,*}

¹ Innovation and Technology Group, Kuwait Oil Company (KOC), Ahmadi P.O. Box 9758, Ahmadi 61008, Kuwait; aqubian@kockw.com (A.Q.); asabbas@kockw.com (A.S.A.); nkhedhair@kockw.com (N.A.-K.); jperes@kockw.com (J.F.P.)

² LUKOIL Neftohim Burgas, 8104 Burgas, Bulgaria

³ Institute of Biophysics and Biomedical Engineering, Bulgarian Academy of Sciences, 1113 Sofia, Bulgaria

⁴ Central Research Laboratory, University Prof. Dr. Assen Zlatarov, 8010 Burgas, Bulgaria

⁵ Department Chemical Technologies, University of Chemical Technology and Metallurgy, 1756 Sofia, Bulgaria

⁶ College of Engineering and Petroleum, Kuwait University, Safat P.O. Box 5969, Safat 13060, Kuwait

⁷ Montreal Oil and Gas Inc., Montreal, QC H2Y 2K9, Canada

* Correspondence: mrriazi@gmail.com

Abstract: The precipitation of asphaltene and waxes occurs when crude oil characteristics change as a consequence of pressure, temperature variations, and/or chemical modifications, etc. The costs associated with the cleaning of deposition on the production equipment and the loss of profit opportunities can go beyond hundreds of millions of USD. Thus, there is a strong incentive to search for ways to mitigate deposit formation during the crude production process. A light crude bottom hole fluid sample from a deep well with an asphaltene deposition problem was analyzed in the laboratory. Basic data on density, viscosity, bubble point, GOR, and asphaltene onset pressure were measured at a PVT laboratory. Asphaltene characterization, as a prescreening for appropriate inhibitors, has been conducted using asphaltene phase diagrams (APD). The APD generated from two developed software programs in both Matlab and Excel codes were favorably compared with the phase behavior of other oil samples available in the literature and has shown to be an excellent match. Various test methods were used to demonstrate the asphaltene instability of the oil samples. Eleven chemical inhibitors from five global companies were screened for testing to inhibit the precipitation. The optimum concentration and the amount of reduction in precipitation were determined for all of these chemicals to identify the most suitable chemicals. Finally, some recommendations are given for the field application of chemicals.

Keywords: crude oil; SARA; asphaltene stability; precipitation; asphaltene inhibitor



Citation: Qubian, A.; Abbas, A.S.; Al-Khedhair, N.; Peres, J.F.; Stratiev, D.; Shishkova, I.; Nikolova, R.; Toteva, V.; Riazi, M.R. Screening and Investigation on Inhibition of Sediment Formation in a Kuwait Light Crude Oil by Commercial Additives with Some Guidelines for Field Applications. *Processes* **2023**, *11*, 818. <https://doi.org/10.3390/pr11030818>

Academic Editor: Andrew Hoadley

Received: 31 January 2023

Revised: 28 February 2023

Accepted: 5 March 2023

Published: 9 March 2023



Copyright: © 2023 by the authors. Licensee MDPI, Basel, Switzerland. This article is an open access article distributed under the terms and conditions of the Creative Commons Attribution (CC BY) license (<https://creativecommons.org/licenses/by/4.0/>).

1. Introduction

Asphaltene precipitation can negatively affect the oil recovery and refining processes from its early stage in the reservoir and during enhanced oil recovery (EOR), to the flow of produced oil in the production well, as well as surface facilities. Through the adsorption of crude oil polar components onto surfaces, asphaltene can alter wettability. It will also block pore spaces, resulting in reduced local permeability and, therefore, reduce oil production rates. The asphaltene deposition can also occur in the production well where the pressure drop is maximum, and the thickness of deposited asphaltene changes over time. If the crude oil is sensitive to the acids used for well stimulation this may cause a decrease in the production rate due to asphaltene precipitation. Furthermore, it is also reported that an increase in asphaltene precipitation has been observed in sections of the well with increases in turbulence in the flow.

Asphaltenes are complex molecules with molecular weights ranging from 1000 to 5000 g/mol and densities of about 1100–1250 kgm⁻³. Asphaltene molecules contain some heteroatoms such as nitrogen, sulfur, and oxygen. They are mainly aromatics and may precipitate at certain thermodynamic conditions such as temperature, pressure, and oil composition. Asphaltene colloid formation, flocculation, and precipitation processes have been studied and reported in the literature [1–4].

The presence of resins plays an imperative role in asphaltene precipitation and deposition. During gas injection into a reservoir for enhanced oil recovery processes, the composition of oil changes, and, consequently, precipitation may occur [5]. In addition to the composition of the crude oil, the type and amount of injected gas, temperature, pressure, flow characteristics, and properties of the conduit (pipeline or production well) will affect asphaltene precipitation. A recent review of asphaltene precipitation and associated problems in production processes were made by Mohamed, et al. [6,7].

Due to the complex nature of asphaltene, the phenomenon of asphaltene precipitation was never fully understood by the researchers despite extensive research conducted in this area over the last several decades. The three main questions for the industry regarding asphaltene deposition are: when it happens, how much precipitation occurs, and how to prevent or reduce the amount of precipitation.

It is important to correctly predict the onset of asphaltene precipitation and deposition. Thermodynamic models developed for the prediction of asphaltene precipitation are composition-dependent and they should be optimized for a given crude. We will use some crude oil samples and will develop a suitable thermodynamic model tuned for similar oils and reservoirs. This paper is focused on experimental measurements for a light crude oil sample, the development of an appropriate thermodynamic model for the phase behavior of the oil, and the determination of the regions of instability. The other major objective of this work was to determine a suitable inhibitor or chemical that can be used to minimize the amount of asphaltene precipitation.

2. Materials and Methods

2.1. Crude Oil Samples and Their Characterization

The oil sample was taken by the operating company from an onshore deep well (referred to as sample A). This was the main sample used for experiments, testing, and evaluation. Three samples, each of 500 mL were taken on 5 June 2018 at a depth of 14,000 ft. The bottom hole pressure and temperature were 4063 psi and 242 °F, respectively. This oil sample was used in the petroleum research facility laboratory at Kuwait University to measure the basic PVT data, as given in Table 1. The bubble point was determined from a constant mass experiment (CME) conducted at 242°. The composition of the sample was determined from PVT and a subsequent GC analysis. A summary of the results is given in Table 1.

Some similar basic data on another oil sample (Sample B) from another well located in the same field are given in Table 2. The composition of oil samples for these oils is given in Table 3.

In addition to the live oil sample, 10 L of dead crude oil was collected by the gathering center which was received in November 2020. Basic measured properties for these oil samples are given in this section. Properties such as API, density, viscosity, sulfur, and asphaltene contents were measured at Lukoil Neftochim Burgas and are given in Table 4 and the true boiling point distribution is presented in Figure 1.

Table 1. General Properties for Oil Sample A at 242 °F.

Reservoir Temperature	242
Sample volume used at reservoir T & P, mL	67.5
Flashed Liquid Volume at STP, mL	47.1
GOR, scf/bbl	675.5
Basic Sediment & Water Content, wt.%	0
Reservoir Initial Pressure, psig	9300
Bubble point pressure, psia	2271.6
Asphaltene onset pressure, psia	5200
Density at reservoir condition, g/cm ³	0.640
Density at 60 F, kg/m ³	823.8
Mol. Wt., g/mol	194
API Gravity	40.1
Absolute viscosity, cP	4.91
Kinematic viscosity at 60 F, mm ² /s (cSt.)	4.04
SARA analysis of STO	
Saturates, wt.%	65.5
Aromatics, wt.%	28.3
Resin, wt.%	4.7
Asphaltene, wt.%	1.6

Table 2. SARA Analysis and BP of Oil Sample B.

Reservoir Temperature, F	230
Asphaltene onset pressure, psia	4500
Bubble point pressure, psia	3130
SARA analysis of STO	
Saturates, wt.%	57.3
Aromatics, wt.%	28.5
Resin, wt.%	3.1
Asphaltene, wt.%	1.0

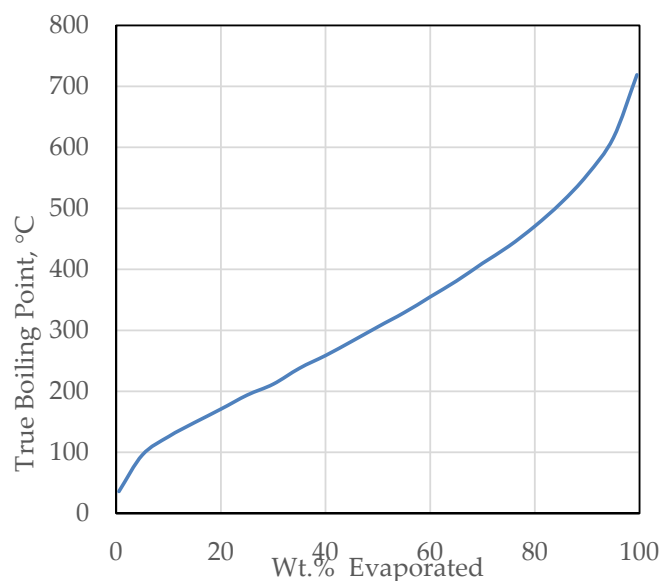
Table 3. Composition of two live oil samples from an oil field in the Middle East.

Component	Sample A mol %	Sample B mol %
CO ₂	2.03	0.90
N ₂	0.12	0.03
H ₂ S	1.91	0.03
C ₁	27.47	41.95
C ₂	12.68	10.68
C ₃	8.23	7.11
nC ₄	3.10	3.48
iC ₄	0.90	0.96
nC ₅	3.41	2.10
iC ₅	2.95	1.22
C ₆	5.36	2.89
C ₇₊	31.84	28.65
MW ₇₊	212	211
SG ₇₊	0824	0.843

The densities at two different temperatures were measured according to the ASTM D4052 test method. The sulfur for each cut was measured according to the ISO 8754 test method. These data are given in Table 5 and presented in Figures 2–4. Simulated Distillation (GC) by ASTM D 7196 is presented in Figures 5 and 6.

Table 4. Basic properties of dead crude oil sample.

Property	Value
Density at 15 °C, g/cm ³	0.8313
Density at 20 °C, g/cm ³	0.8277
API Gravity, 60 °F/60 °F	39.29
Sulfur content, wt.%	1.049
C ₅ asphaltenes, wt.%	2.6
C ₇ asphaltenes, wt.%	1.6
Kin. Viscosity at 40 °C, mm ² /s	9.4

**Figure 1.** TBP Distribution for the crude oil sample. Test Methods: ASTM D2892 and ASTM D 5236.**Table 5.** Density and sulfur contents of narrow cuts. Test Methods: Density: ASTM D4052. Sulfur: ISO 8754.

Narrow Cuts BP, °C	Density g/cm ³		Content of Sulfur, wt.%
	at 15 °C	at 20 °C	
IBP-70 °C	0.6496	0.6447	0.060
70–100 °C	0.6949	0.6902	0.048
100–110 °C	0.7170	0.7124	0.061
110–130 °C	0.7302	0.7256	0.058
130–150 °C	0.7503	0.7458	0.063
150–170 °C	0.7675	0.7630	0.073
170–180 °C	0.7775	0.7733	0.070
180–200 °C	0.7857	0.7819	0.073
200–220 °C	0.7952	0.7914	0.077
220–240 °C	0.8029	0.799	0.107
240–260 °C	0.8160	0.8123	0.224
260–280 °C	0.8307	0.8271	0.466
280–300 °C	0.8442	0.8406	0.677
300–320 °C	0.8482	0.8446	0.787
320–340 °C	0.8638	0.8602	1.252
340–360 °C	0.8820	0.8784	1.831
>360 °C			
360–380 °C	0.8885	0.8812	1.824
380–390 °C	0.8949	0.8916	1.815
390–430 °C	0.9000	0.8967	1.716
430–470 °C	0.9163	0.9132	1.876
470–490 °C	0.9291	0.9261	2.047
490–500 °C	0.9377	0.9347	2.248
>500 °C	0.9828	0.9802	3.025

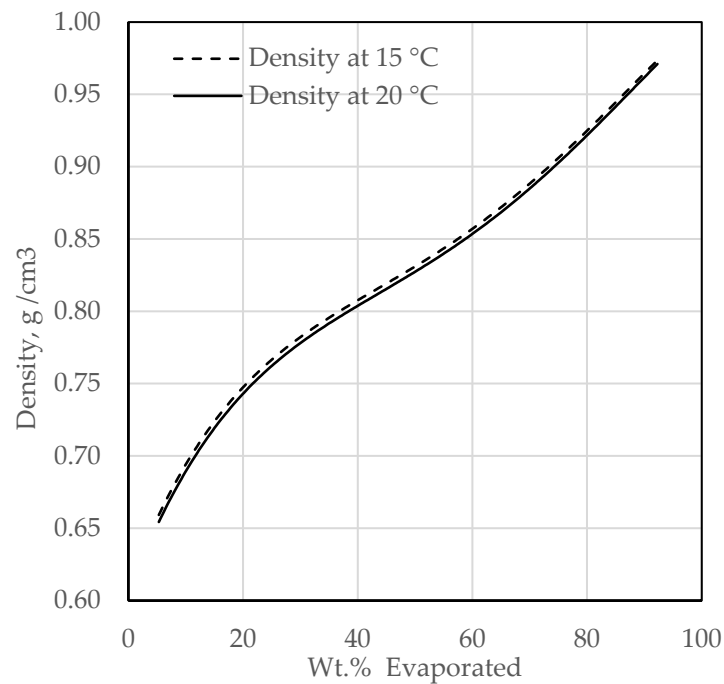


Figure 2. Density of crude cuts at 15 °C and 20 °C.

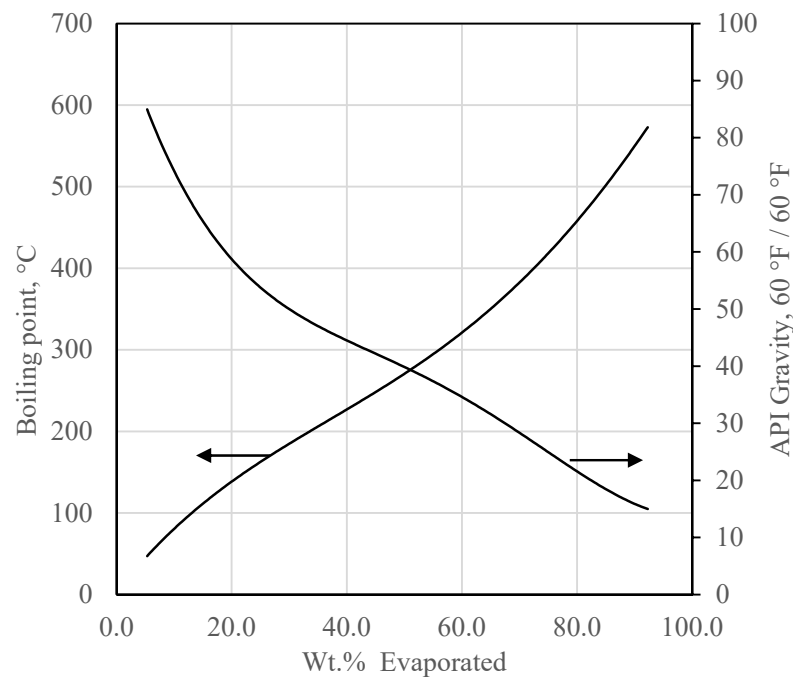


Figure 3. API gravity and boiling point of narrow cuts.

2.2. Asphaltene Stability Test Methods

The asphaltene stability test methods employed in this study are itemized below:

- Method I: asphaltene/resin ratio deduced from a SARA analysis as described by Yen et al. [8];
- Method II: colloidal instability index (CII) defined based on SARA analysis as explained in [8] and shown by Equation (1):

$$\text{CII} = \frac{\text{Saturates (wt.\%)} + \text{Asphaltenes (wt.\%)}}{\text{Aromatics (wt.\%)} + \text{Resins (wt.\%)}} \quad (1)$$

- Method III: asphaltene stability test by the Stankiewicz method explained in detail in [9];
- Method IV: based on the method suggested by Yen et al. [8] based on SARA analysis, where the graph of the Y-X diagram is prepared with Y = Asphaltenes + Saturates; and X = Aromatics + Resins;
- Method V: based on the method suggested by de Boer et al. [10]. It employs the difference between initial pressure and bubble point pressure and the density of reservoir fluid under reservoir conditions.

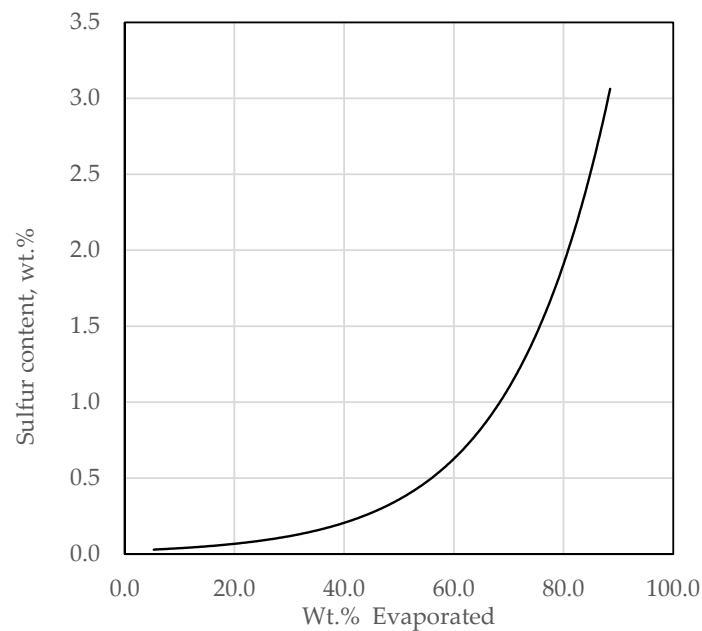


Figure 4. Sulfur content of narrow cuts, wt.%.

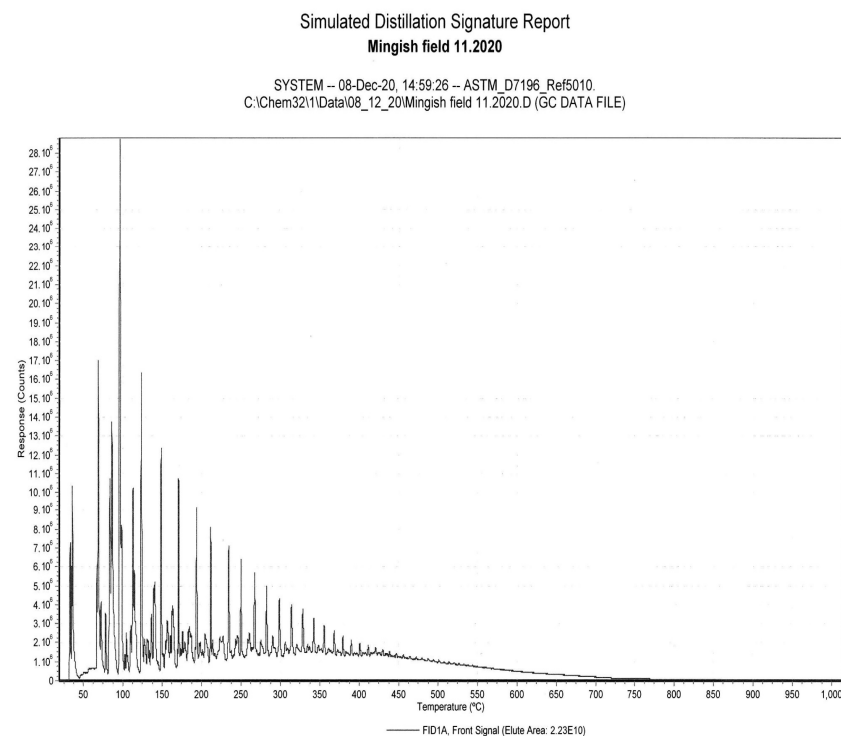


Figure 5. Simulated Distillation (GC) by ASTM D7196 for Crude Sample A.

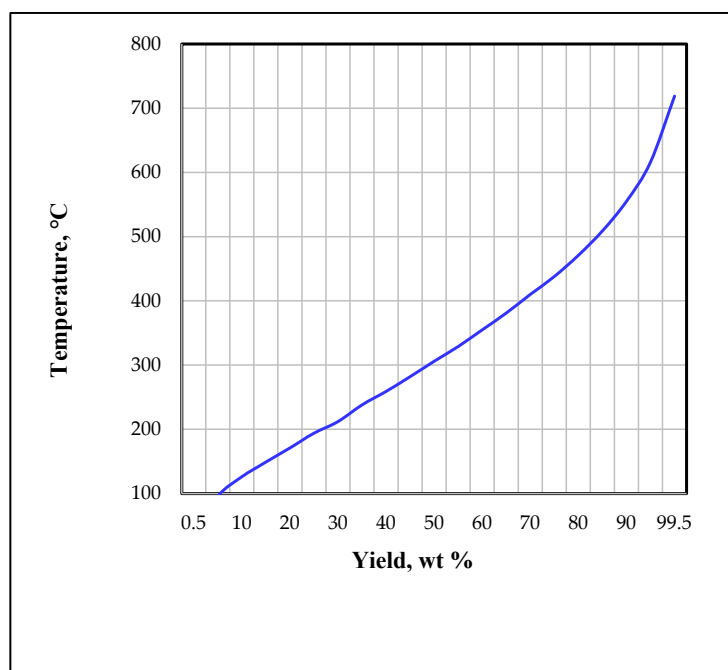


Figure 6. Simulated Distillation (GC) Graph for the Crude Oil Sample A.

2.3. Regions of Asphaltene Instability

Once it has been determined that an oil sample is unstable, based on the methods discussed in the previous section, it is important to determine the region in the phase diagram where asphaltene precipitation can occur. This can be done through an asphaltene phase diagram (APD). Generation of an APD is the key to determining under what conditions asphaltene formation occurs. Perturbed chain statistical associating fluid theory (PC-SAFT) is a rather advanced approach to the estimation of the behavior of a complex mixture originally proposed by Chapman et al. [11], and later modified by Gross and Sadowsky [12]. Cubic-plus-association equation of state (CPA-EOS) is also another class of EOS, which takes into account the association between the molecules. Chapman and his group at Rice University over the last two decades showed that PC-SAFT is quite suitable for estimating the asphaltene–crude oil PVT behavior [13–17]. They particularly proposed a thermodynamic framework based on PC-SAFT EOS to predict asphaltene phase behavior and named the tool the asphaltene deposition tool (ADEPT) [13]. According to Gross and Sadowsky, the total compressibility factor can be calculated as the sum of the ideal gas, hard chain, and dispersion contributions, as follows [12]: $Z = Z^{id} + Z^{hc} + Z^{disp}$. In the PC-SAFT framework, three parameters of segment number in a chain (m), the segment diameter (σ), and segment energy (ϵ/k) are used to differentiate components. So far, researchers have proposed different methods for the estimation of these parameters [11]. There exist a few correlations that are mostly used for asphaltene precipitation modeling, as reported by Gonzalez et al. [15] which can be used for calculating the PC-SAFT parameters of petroleum cuts and fractions.

In this work, the PC-SAFT approach of neglecting the association term was used to develop software for the asphaltene phase equilibria calculation of some Kuwaiti oil samples. Two software were developed, one with Matlab and one fully with Excel VBA code. The Matlab version is faster as it uses its internal optimization tool while for Excel, we developed our own optimization in the VBA codes. The input data for each oil sample is fluid composition, SARA analysis, bubble point, and or onset pressure at least at the reservoir or bottom hole temperature (BHT). For gas injection processes, an option for the amount of injected gas is provided. Experimental data on bubble point and/or upper asphaltene onset pressure (UAOP) can be used to get optimized values for the aromaticity and molecular weight of the asphaltene component of the oil sample. These parameters

need to be determined only once for each crude sample, and for all subsequent calculations, there is no need for this optimization step. When optimized parameters are used, the calculations in Excel are quite fast (similar to Matlab) and calculations are performed in less than 30 seconds. A schematic of the flow diagram for the calculation of asphaltene onset and bubble point pressures is shown in Figure 7.

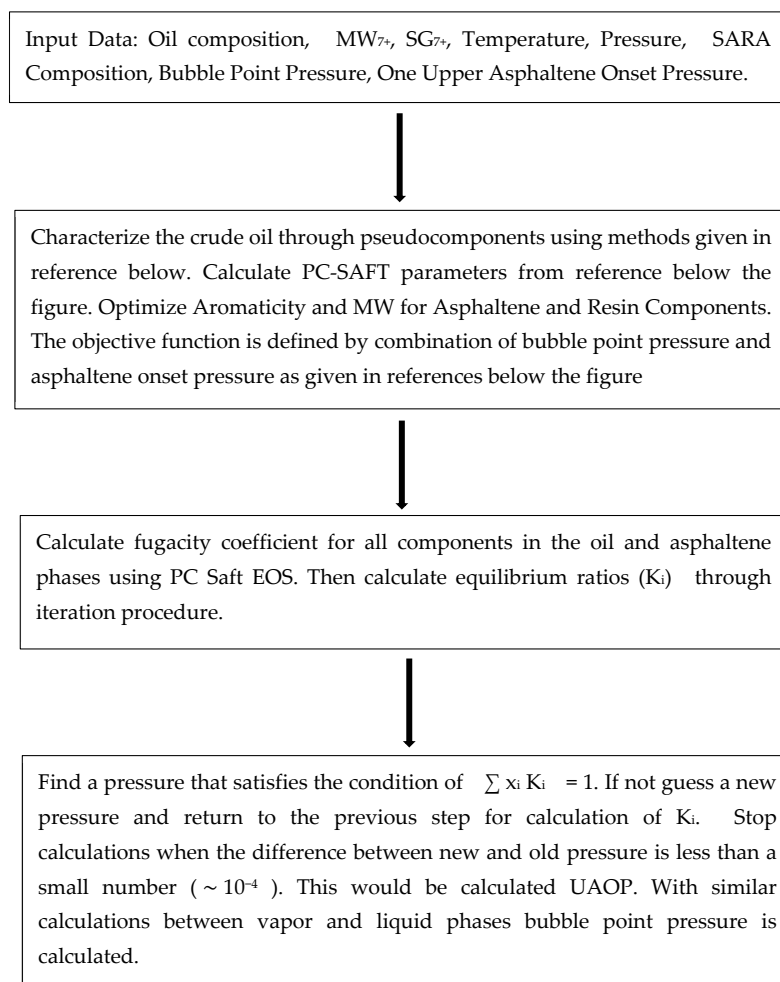


Figure 7. A summary of calculation procedure for the bubble point and upper asphaltene onset pressures. Characterization method taken from Reference [1], PC-SAFT parameters from [15], optimization procedure from [13,16–18].

2.4. Screening of Chemical Inhibitors for Retardation of Asphaltene Precipitation

The asphaltene flow assurance problem can be handled in three different ways: (one) to prevent it from happening, (two) to reduce the extent of precipitation, and (three) to dissolve deposited asphaltene. It is interesting to know that if the asphaltenes in the produced fluid are in the stable dispersion form, they will not harm the production through permeability reduction, although they will increase the oil–solid mixture viscosity. The extent of asphaltene precipitation can be controlled by not allowing the size of the asphaltene aggregate to grow. For example, the adsorption of nonionic dispersants onto the surface of an asphaltene particle can avoid its growth and, therefore, will limit the size of the aggregate, which in turn will allow the asphaltene to be carried along the oil phase [19].

There are clearly two groups of chemical additives that can prevent asphaltene deposition. They are ADs (asphaltene dispersants) and asphaltene inhibitors (AIs). Examples of nonpolymeric ADs are the very low polarity alkylaromatics or the alkylaryl sulfonic acids. Examples of AIs are the alkylphenol/aldehyde resins and similar sulfonated resins, polyolefin esters, amides or imides with alkyl, alkylphenyl or alkylene-pyridyl functional

groups, and alkenyl/vinyl pyrrolidone copolymers. AIs are not effective in formations but are mainly used in wellbores and surface equipment. AIs increase the asphaltene stability under wider operation conditions while ADs reduce the particle size and keep particles in suspension form in the oil. These chemicals are oil-specific. For example, the presence of nitrogen in asphaltene can interact with the polymeric inhibitors containing H+ atoms such as hydroxyl groups. In general, AIs are polymeric-type chemicals and to be effective we must reach a certain critical concentration while ADs act almost proportionately to concentration. AIs can be best applied upstream of the bubble point pressure which is commonly downhole to prevent asphaltene flocculation. It is recommended to use either an AI or an AD, but not both. The use of live oils and dead oils in testing AIs and ADs may give different results, however, tests with dead oil can be used for general screening of AIs or ADs since the trends of effectiveness are similar to those with live oils. More specific information about the properties and effectiveness of these chemical additives is given by Kelland [19].

When an inhibitor is used to reduce asphaltene deposition, we need to determine its performance by measuring the amount of deposit before and after a dispersant is used. Methods of deposit test level are fully described in the literature [20–35]. The asphaltene dispersant test (ADT) method has been used in this study to determine the effectiveness of an inhibitor in reducing asphaltene deposition as described in our earlier study [26] and adopted from [27]. Once the mass of asphaltene before and after the addition of an inhibitor is measured, the efficiency can be calculated from the following equation:

$$\text{Efficiency (\%)} = \frac{\text{Volume of asphaltene deposit before inhibitor} - \text{Volume of Asphaltene deposit after inhibitor}}{\text{Volume of asphaltene deposit before inhibitor}} \times 100 \quad (2)$$

The effect of the use of inhibitors to suppress sediment formation was examined by employing an asphaltene dispersant test (ADT), as described in [27]. The oil sample is mixed with large amounts of heptane to obtain a clear sample that allows sediment observation through it. During this study, the crude oil sample A and the H-Oil ATB samples were mixed with n-heptane in an amount of 93%. The blend of 7% oil/93% n-heptane was placed in a graduated centrifuge tube and then centrifuged at 5000 rpm for 30 min. A sample of the oils with no dispersant was used as a control. The commercial additives were mixed with the studied oils and then homogenized in a closed beaker for a period of one hour using a magnetic stirrer at 700 rpm. Then, three grams of crude oil sample A (0.5 grams of H-Oil VTB samples) with the additive were placed in a graduated centrifuge tube and mixed with 40 grams of n-heptane, and after that centrifuged at 5000 rpm for 30 min. Reading the volume of the sediment from the graduated centrifuge represents the amount of the sediment formed at the conditions studied. The sediment volume of the pure crude oil sample A was 0.12 mL, while those of the pure H-Oil ATB samples were 0.40, and 0.45 mL. The relative error of the measurement of the sediment volume was found to be 11.0%.

3. Results

3.1. Results from Asphaltene Stability Test Methods

One simple method to judge the oil colloidal stability is to calculate the ratio of saturates/aromatics from SARA analysis. This ratio is an indirect measure of the solvating power of an oil sample for asphaltenes (a high ratio implies poor solvating power). The asphaltene/resin ratio, on the other hand (Method I), relates to the measure of colloidal stability of the asphaltenes (ratio of asphaltene/resin implies good colloidal stabilization). Oils with higher resin content are more stable with the addition of a solvent such as n-C₅ or n-C₇. Another simple method is to determine a parameter known as the colloidal instability index (CII) defined based on SARA analysis as described by Yen et al. [8]. If CII is less than 0.7, the oil is stable and if greater than 0.9, it is unstable. If CII is between 0.7 and 0.9, the oil is mildly unstable (Method II). In addition to these methods, there are three other graphical methods. Method III was proposed by Stankiewicz, et al. [9] and Method V is based on the difference between the initial pressure and the bubble point pressure applied to crude oil

sample A, as shown in Figure 8a,b, respectively. Another method proposed by Yen et al. [8] shows three regions of unstable, mildly stable, and stable regions from the correlation of SARA data (Method IV). Results obtained from all these methods are consistent with each other. For example, as shown in Figure 9a,b, when Methods III and IV were used to test oil sample B, both methods showed that the crude oil sample is unstable. For the oil in sample B (Table 2), the ratio of asphaltenes/resins is 0.337, which is greater than 0.3, and based on Method I, the oil is unstable. Similarly, the colloidal instability index (CII) based on Method II was calculated for this oil as 2.03, which is greater than 0.9, and, thus, the oil is unstable. As a result, both crude oil samples were unstable according to all these five stability test methods.

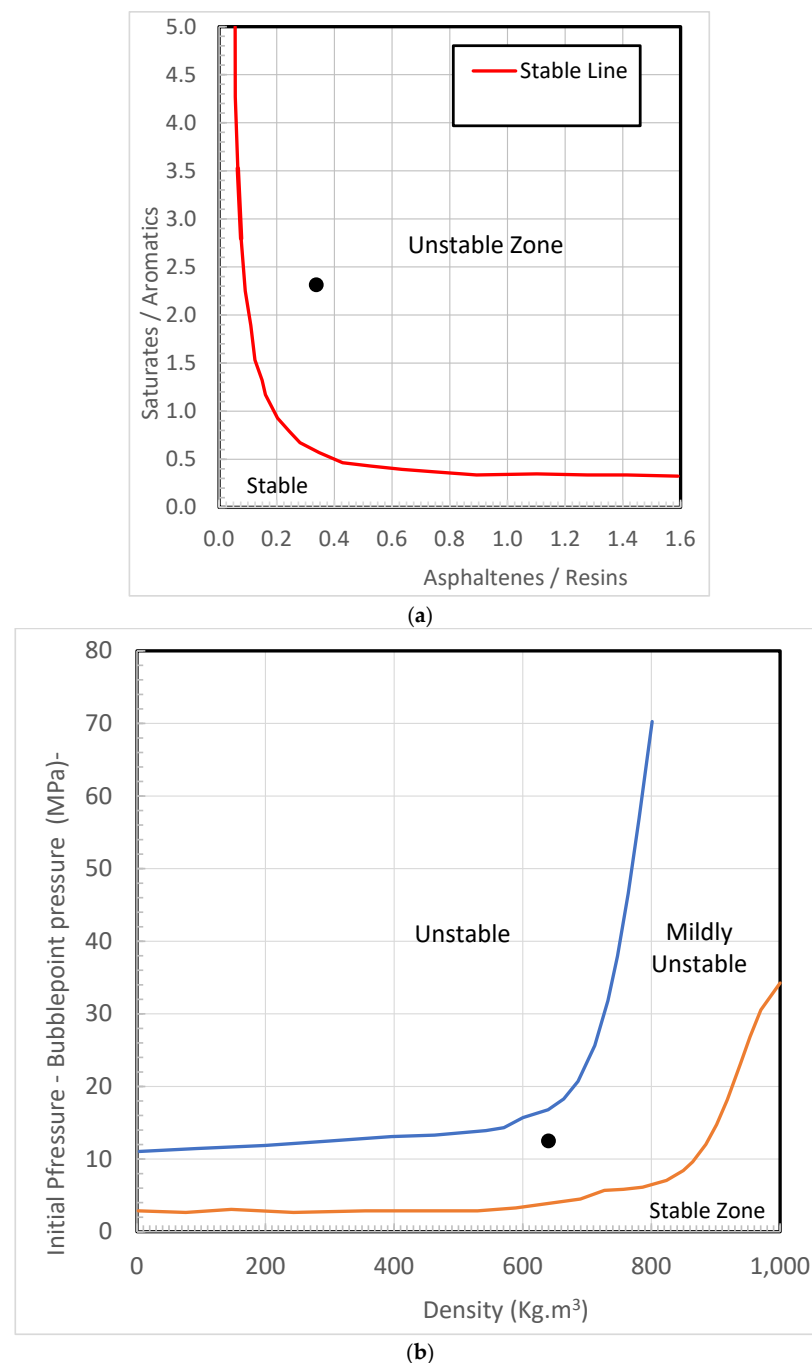
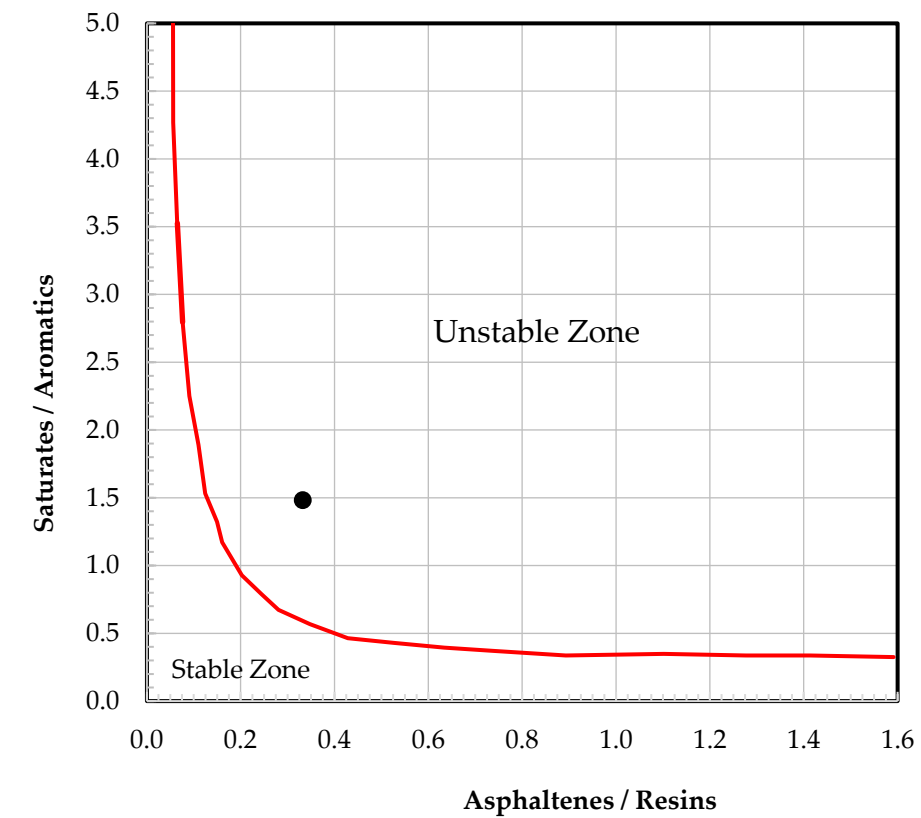
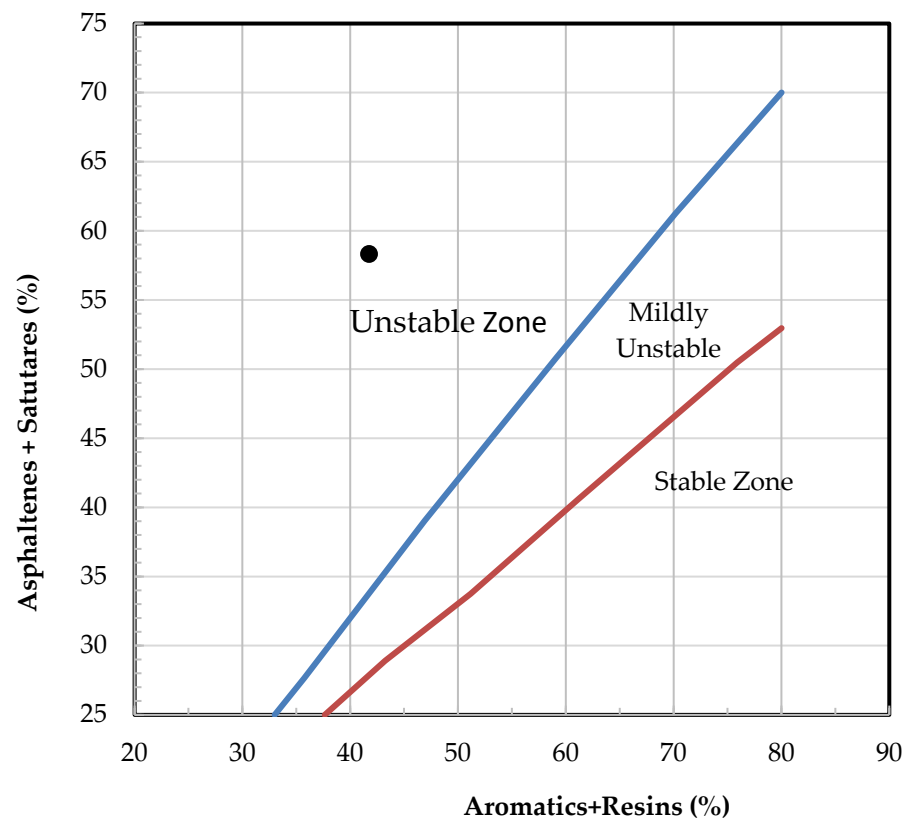


Figure 8. (a). Asphaltene Stability Test Method III Applied to Oil Sample A. (b). Asphaltene Stability Test Method V Applied to Oil Sample A.



(a)



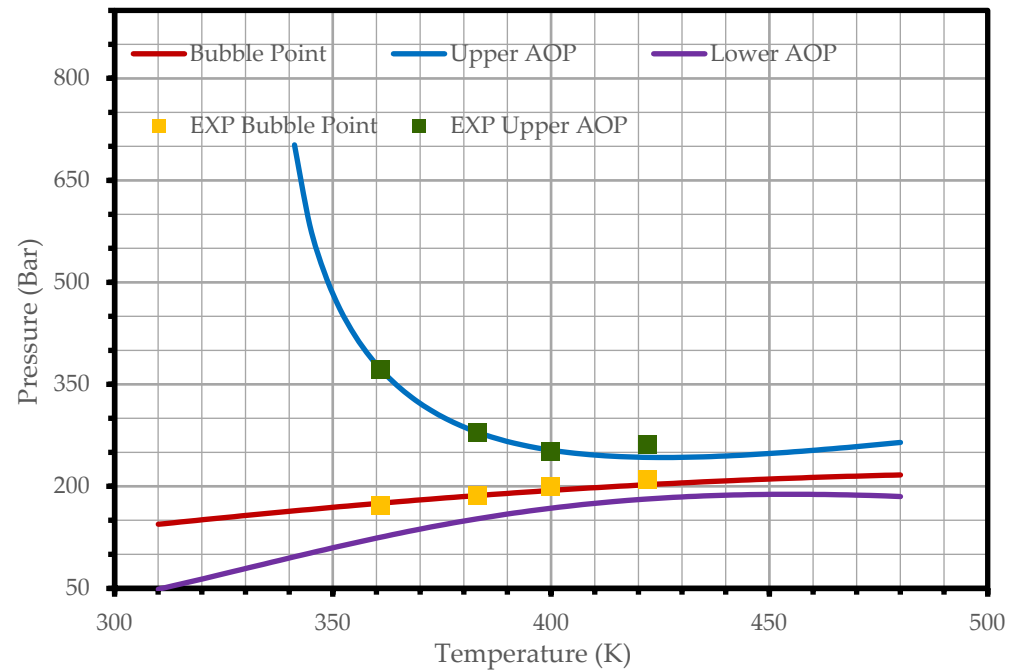
(b)

Figure 9. (a) Asphaltene Stability Test by Stankiewicz et al. [9] method (Method III) for the Oil Sample B (Table 2). (b) Asphaltene Stability Test by Yen's Method (Method IV) for the Oil Sample B.

3.2. Determination of Regions of Asphaltene Instability for the Studied Crude Oil Samples

To evaluate our program, described in Section 2.3 in this work, we used ADEPT [13] of the Chapman group at Rice University with several oil samples, and a good agreement was observed, as shown in Figure 10. A similar agreement was observed when tested with other oil samples in which the ADEPT results were available in the literature.

a- APD Results Using Jamaluddin Oil



b- ADEPT-Gonzalez Results using Jamaluddin Oil

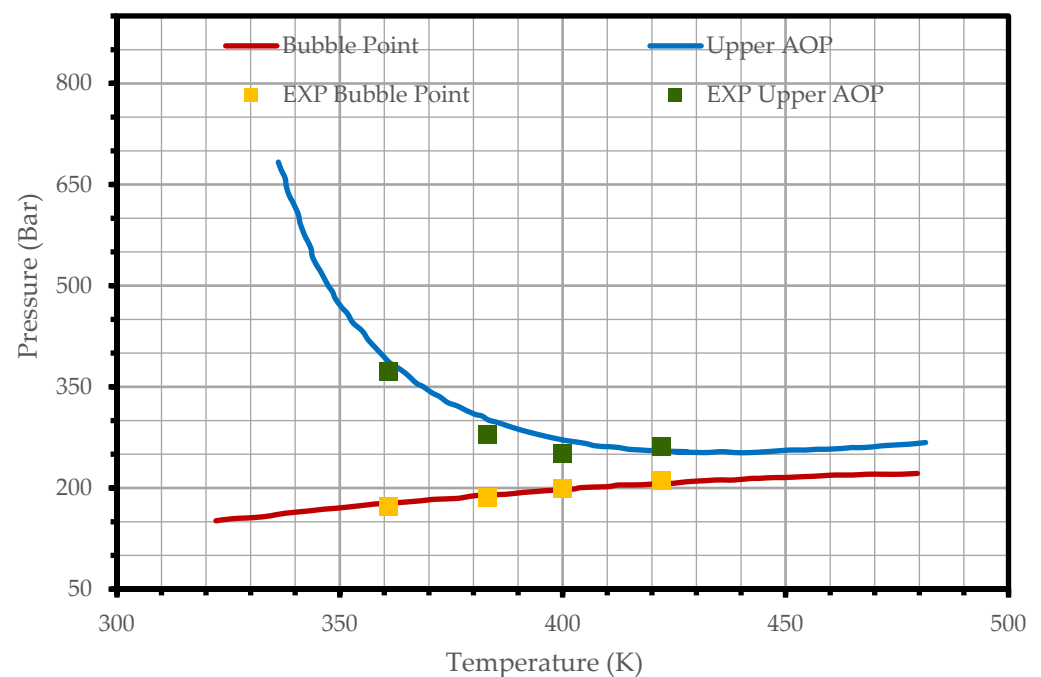


Figure 10. Evaluation of APD program (a) with ADEPT model (b) using oil data from Jamaluddin et al. [29].

An asphaltene phase diagram for oil sample A is given in Figure 11 and for oil sample B in Figure 12. The impact of injecting CO₂ gas on APD for oil sample A is shown in Figure 13 for 20% CO₂ injection. By comparing Figures 11 and 13, one can see that by adding CO₂ to the oil, the unstable region increases to a wider condition.

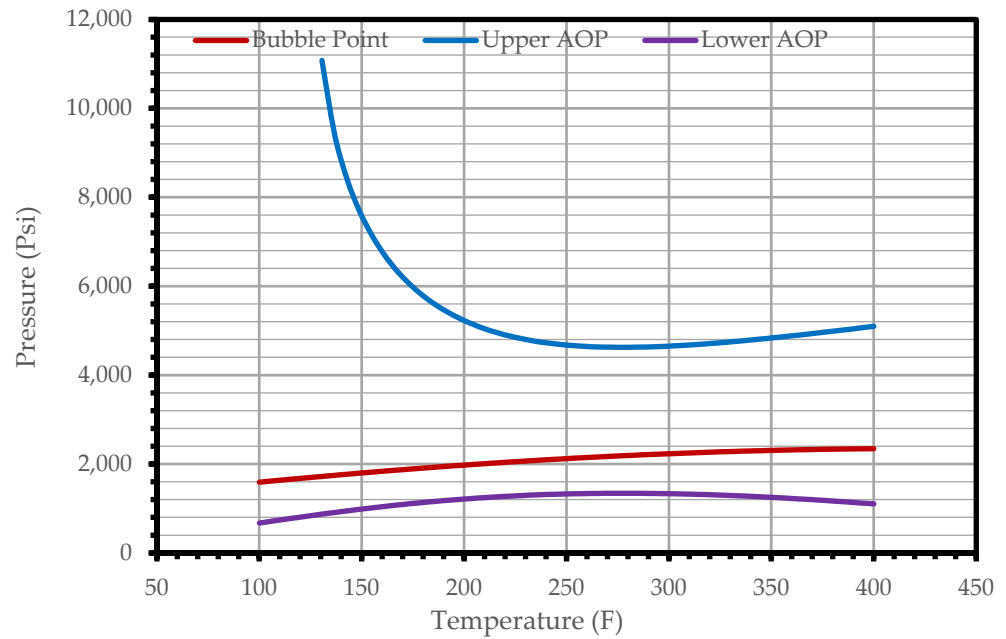


Figure 11. Asphaltene phase diagram (APD) for oil Sample A (in Table 3).

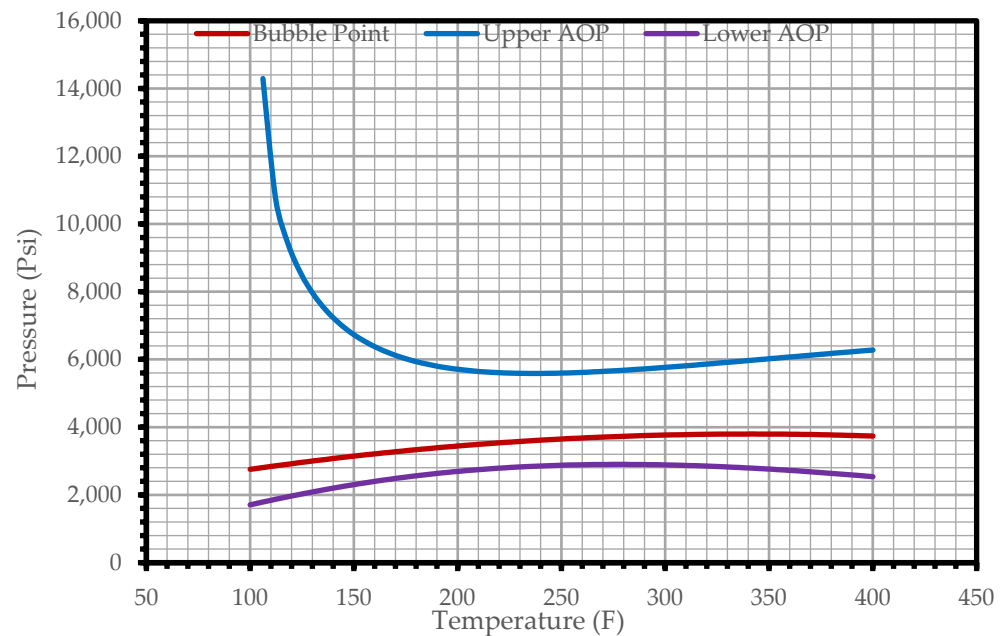


Figure 12. Asphaltene phase diagram (APD) for oil Sample B (in Table 3).

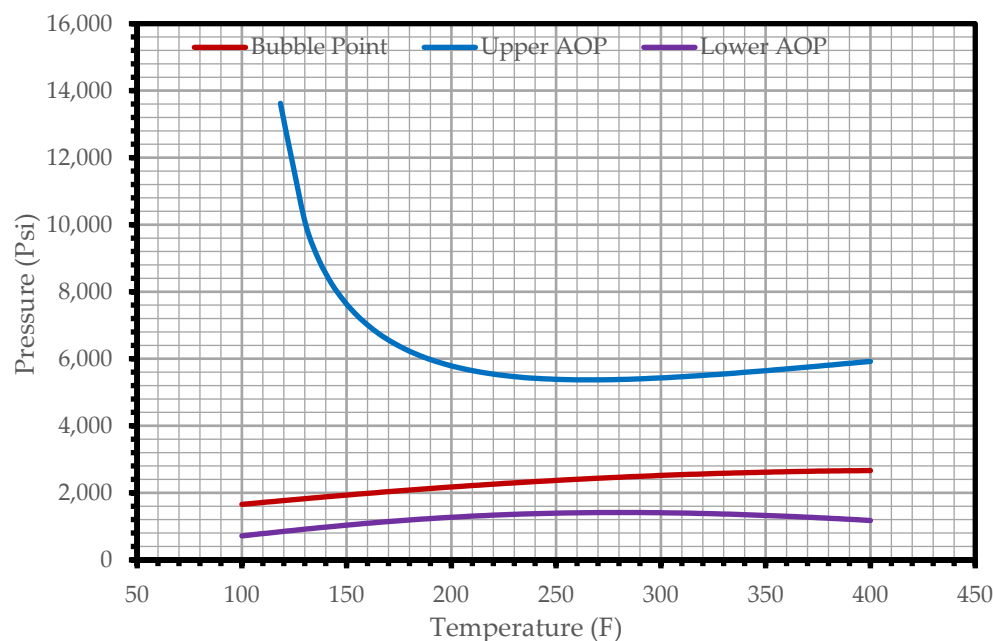


Figure 13. Asphaltene phase diagram (APD) for oil Sample A with 20% CO₂ (see Figure 11 for no CO₂).

3.3. Retardation of Asphaltene Precipitation by the Use of Chemical Additives

Eleven chemical additives employed to retard sediment formation, manufactured and supplied by five major companies around the world, were selected to be used in this study. These chemicals and additives are used for the inhibition, dispersion, and dissolving (dissolution) of asphaltene as well as other types of solid deposition from petroleum fluids with applications in production fields.

The scarce information provided by the supplier indicates that the 11 chemical additives may contain amines in the aromatic solvent, poly-iso-butylene succinimide, polymer in an aromatic solvent, phosphonothioic acid, poly-isobutenyl derivatives, esters with penta-erythritol, alkenyl thio phosphorous ester, formaldehyde, polymers with branched 4 nonylphenol, ethylene-diamine, phosphoric acid, 2-ethyl-hexyl ester, C24-36 alkene, alpha-polymers with maleic anhydride, organic acid derivative, and 1,2,4 trimethylbenzene. The individual additives present a blend of the chemical substances mentioned above in a proprietary and confidential ratio. They are labeled as A1, A2, A3, A4, A5, A6, A7, A8, A9, A10, A11. In order to get some insight into the chemical nature of these 11 additives, infrared (IR) analysis was performed. The IR spectra of the 11 additives are presented in Figures S1–S13. The data from Figures S1–S7 suggest that the additives A1, A2, A3, A4, A5, and A6 pertain to the group of organic acid derivatives. The additives A1, A2, A3, A4, A5, and A6 have the same valence oscillations, however, in different ratios, suggesting a different ratio of the active components in the distinct additives. Figure 14 presents graphs of precipitate volume versus inhibitor concentration for the additives A1–A6 treatment of the crude oil in sample A.

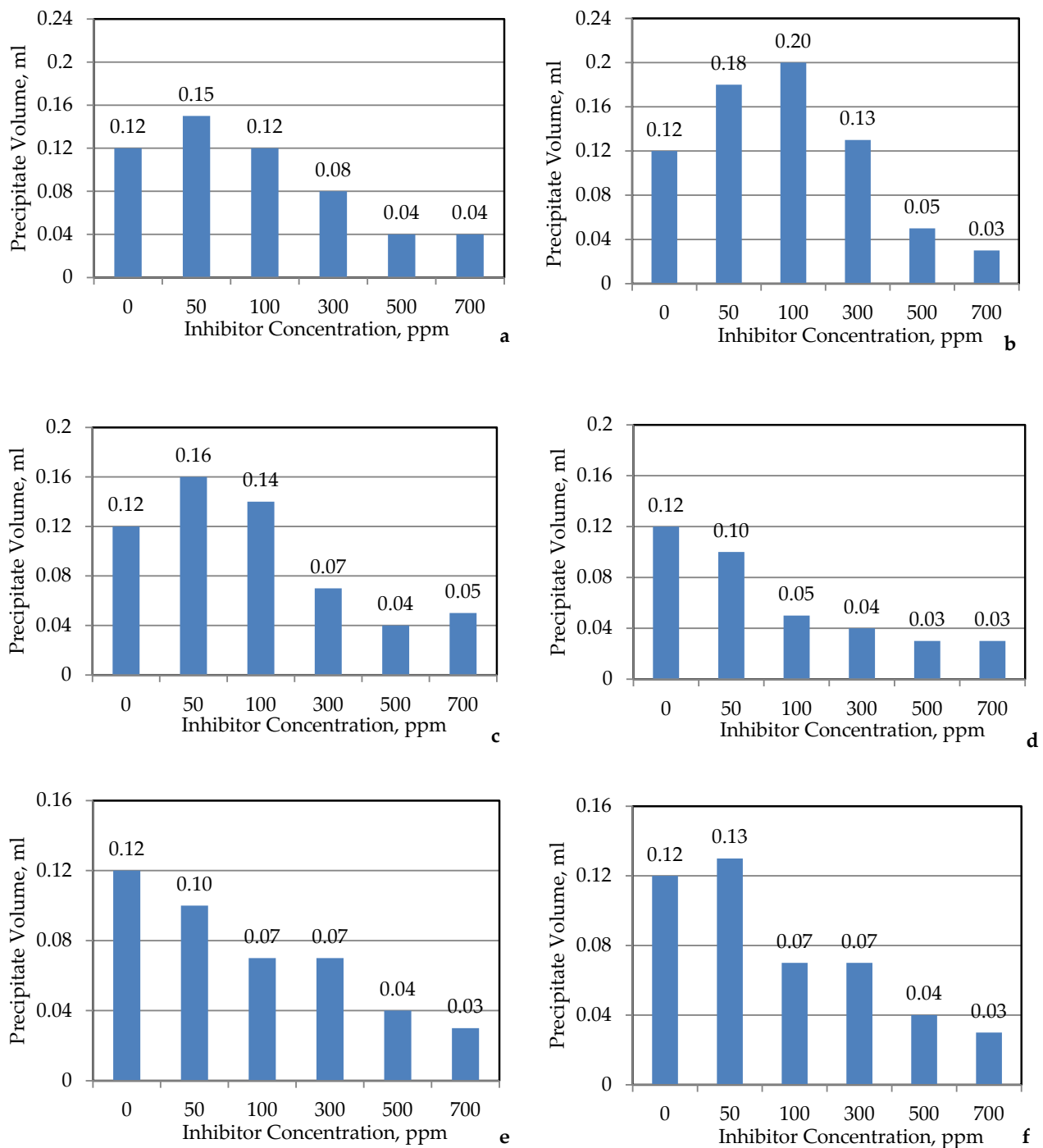


Figure 14. Amount of deposit versus treating rate of inhibitors A1 (a), A2 (b), A3 (c), A4 (d), A5 (e), and A6 (f) (treated crude oil sample A).

Figure 15 presents graphs of precipitate volume versus inhibitor concentration for the additives A7–A11 treating the crude oil in sample A.

Figure 16 presents graphs of precipitate volume versus inhibitor concentration for the additives A2 (a), A3 (b), A4 (c), A5 (d), A7 (e), and A8 (f) with H-Oil hydrocracked atmospheric residue (H-Oil ATB)—sample 1 was treated with additives A2, A3, A4, and H-Oil ATB. Sample 2 was treated with additives A5, A7, and A8—Table 6.

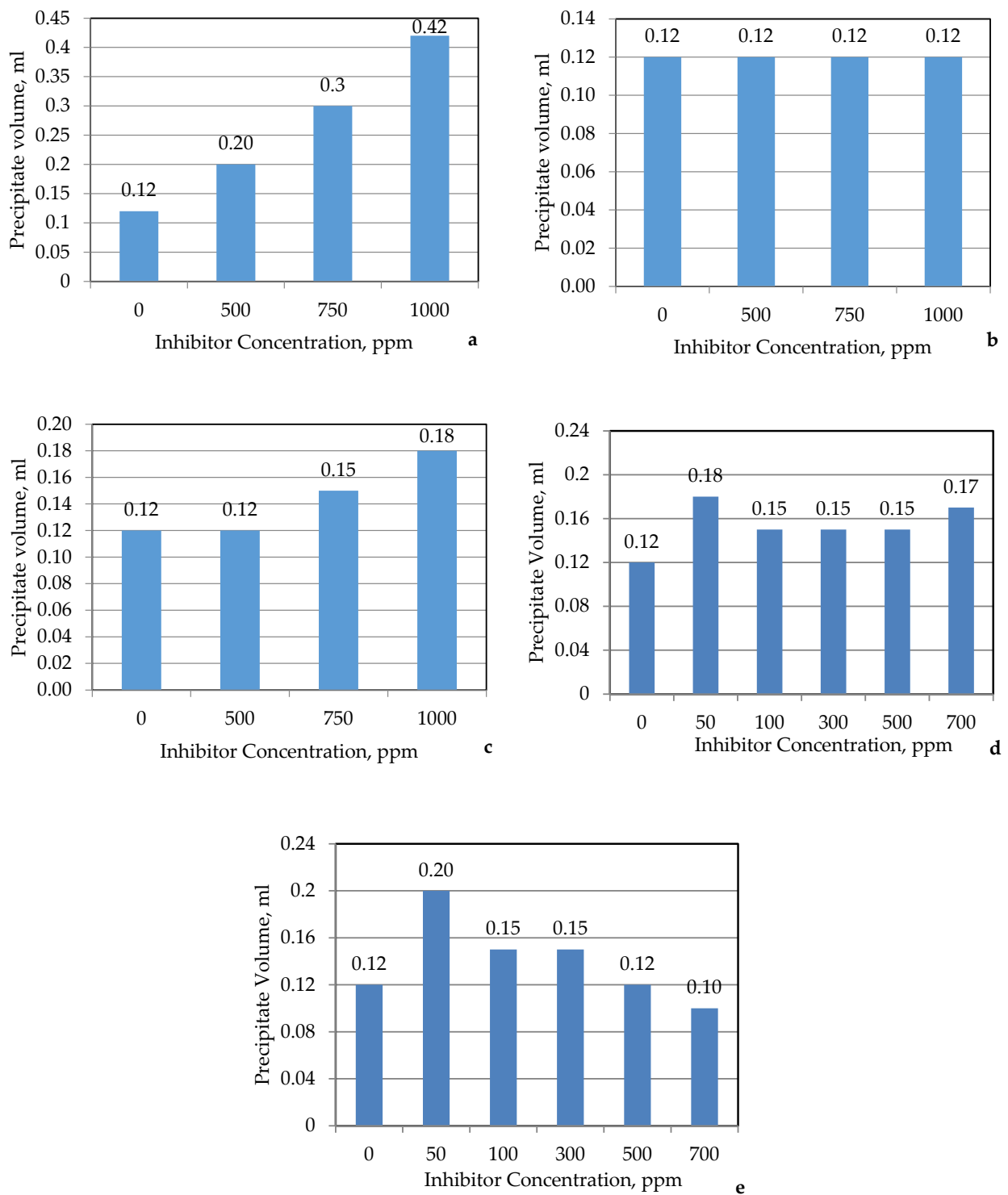


Figure 15. Amount of deposit versus treating rate of inhibitors A7 (a). A8 (b), A9 (c), A10 (d), and A11 (e) (treated crude oil sample A).

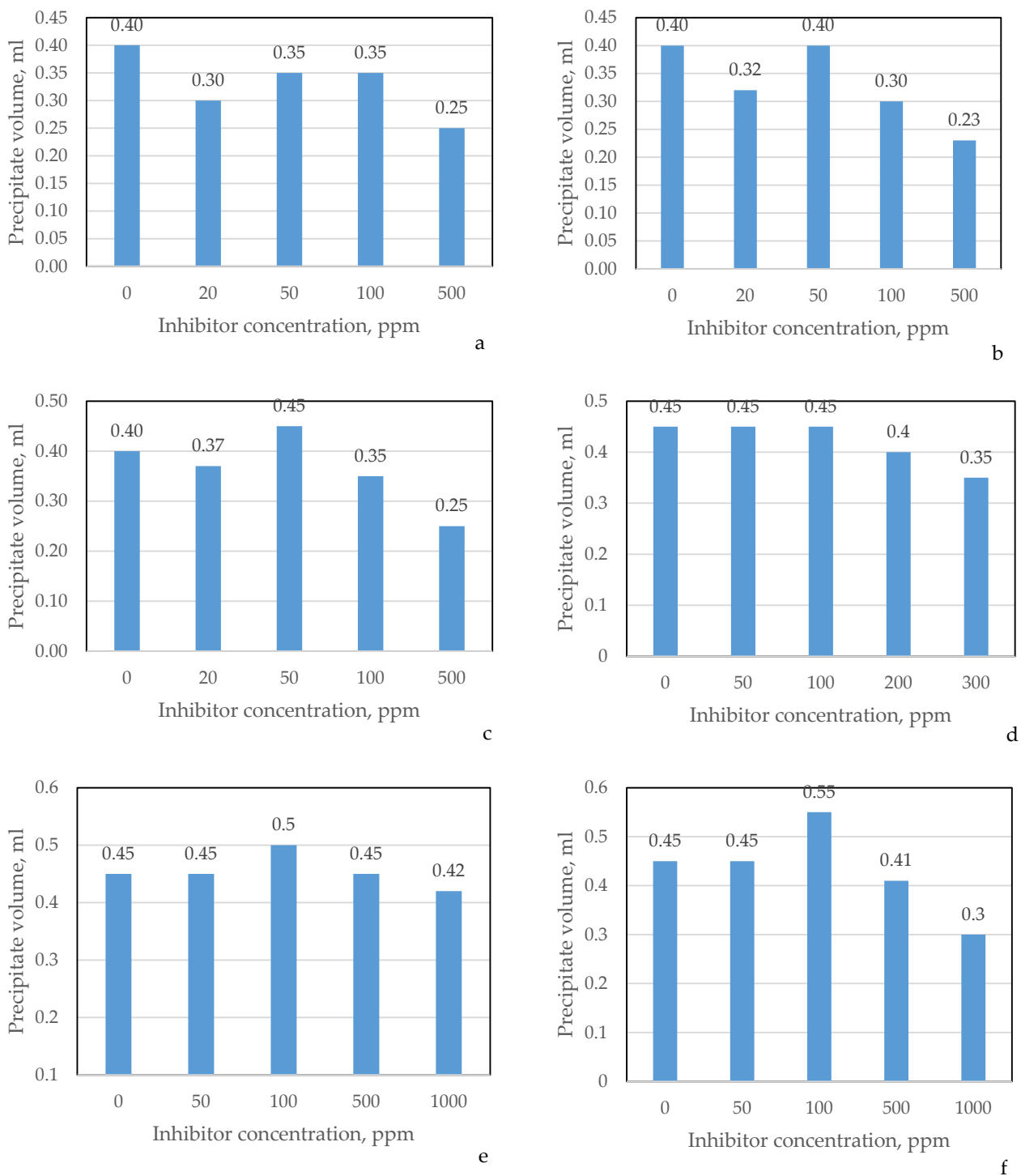


Figure 16. Amount of deposit versus the treating rate of the inhibitors A2 (a), A3 (b), A4 (c), A5 (d), A7 (e), and A8 (f) with H-Oil hydrocracked atmospheric residue (ATB)—sample 1 treated with additives A2, A3, A4, and ATB. Sample 2 treated with additives A5, A7, and A8—Table 6.

The optimum concentration and amount of reduction in a solid deposition for the tested chemicals with crude oil sample A are given in Table 7.

Table 6. SARA Analysis and BP of Oil Sample C.

Properties	H-Oil ATB (68%Urals/32BL) 15.10.2018 Sample-1	H-Oil ATB (80%Urals/20BL) 15.10.2018 Sample-2
H-Oil VR conversion, wt.%	73.6	72.9
Specific gravity SG ₄ ²⁰	1.027	1.012
SARA analysis		
Saturates, wt.%	28.9	31.4
Aromatics, wt.%	59.4	56.8
Resin, wt.%	3.7	4.5
Asphaltene, wt.%	8.0	7.3
Colloidal instability index	0.58	0.62

Table 7. Ranking of the commercial Inhibitors for crude oil Sample A.

Performance Ranking Order	Inhibitor ID	Figure No. for Performance Test	Optimum Concentration ppm	Optimum %Reduction in Precipitate
1	A4	Figure 13d	500 ppm	75%
2	A5	Figure 13e	700 ppm	75%
3	A6	Figure 13f	700 ppm	75%
4	A2	Figure 13b	700 ppm	75%
5	A3	Figure 13c	500 ppm	67%
6	A1	Figure 13a	500 ppm	67%
7	A11	Figure 14e	700 ppm	17%
8	A8	Figure 14b	500 ppm	0% (no effect)
9	A10	Figure 14d	700 ppm	+42% (increasing precipitation)
10	A9	Figure 14c	700 ppm	+50% (increasing precipitation)
11	A7	Figure 14a	1000 ppm	+250% (increasing precipitation)

The optimum concentration and amount of reduction in a solid deposition for the tested chemicals with the H-Oil ATB samples are given in Table 8.

Table 8. Ranking of the commercial inhibitors for H-Oil ATB samples.

Performance Ranking Order	Inhibitor ID	Figure No. for Performance Test	Optimum Concentration ppm	Optimum %Reduction in Precipitate
1	A3	Figure 15b	500 ppm	42%
2	A2	Figure 15a	500 ppm	38%
3	A4	Figure 15c	500 ppm	38%
4	A8	Figure 15f	1000 ppm	33%
5	A5	Figure 15d	300 ppm	22%
6	A7	Figure 15e	1000 ppm	4%

It is interesting to note here that while with the crude oil sample A, additive A8 had no effect on the reduction of the precipitation volume. For the case of H-Oil ATB sample-2, the precipitated volume was reduced by 33%. Additive A7 showed a promotion effect on the precipitation volume of crude oil sample A, whereas, with H-Oil, ATB sample-2 exhibited no effect. The findings in our study are in line with the reports of Mahdi et al. [22], Melendez-Alvarez et al. [27], and Barsenas et al. [30] that the asphaltene dispersants can promote sediment formation depending on the oil treated, chemistry of the additive, medium, and the concentrating range. Barsenas et al. [30] showed in their study that the same asphaltene aggregation inhibitors at lower concentrations inhibited the asphaltene agglomeration while increasing their treatment rate and their efficacy diminished significantly. They found that the same inhibitor during the changing of the medium (from toluene at 50 °C to

o-dichlorobenzene at 90 °C) the asphaltene inhibitor turned into an asphaltene aggregation promoter [30]. They suggested that the inhibitor molecules (i) significantly self-associated in the more polar solvent (o-dichlorobenzene), which could be a reason for the asphaltene adsorption (and enhanced agglomeration) on the surface of such inhibitors and (ii) self-associate occluding their head polar part in the less polar solvent (toluene), which might be a reason for the reduction in inhibitor adsorption on the asphaltene surface and worsening of the inhibition efficiency [30].

3.4. Optimum Inhibitor Concentration at the Field and Impact of Water Cut

The optimum concentrations reported in Table 7 were obtained from laboratory tests conducted at room conditions and with a dead crude oil sample. The conditions at the field are quite different, specifically with the following parameters:

- Temperature;
- Pressure;
- Fluid composition (presence of lighter components);
- Flow rate;
- Water (water cut);
- Concentration of salt and metals in the brine such as Al^{3+} and Fe^{3+} in water.

The temperature of the fluid in the well is higher than the lab temperature. At higher temperatures, the solubility of asphaltene in the oil increases, and this will result in less precipitation and deposition at the field. Furthermore, at higher pressures, the asphaltene stability in the oil increases, as is demonstrated in the APD of Figure 11. Another important factor is the amount of water cut in the wellbore. Generally, as the percentage of water cut increases, the amount of deposition decreases. With a high water cut, the oil is emulsified in water. A high amount of water may turn the wellbore to become water wet and asphaltene deposition may significantly be reduced. However, for the case of well A, the water cut is low at 5%. Furthermore, the flow of oil can cause a reduction in asphaltene precipitation and, as shown by Kor and Kharrat [31], with an increase in oil velocity, asphaltene deposition on the wall decreases. All these factors contribute to a reduction in the amount of inhibitor when applied in a production well. As a rule of thumb, it is believed that the amount of asphaltene deposition in the wellbore is about 30% less than those given in Table 7. Therefore, the optimized dosage in the field is expected to be in the range of 200–300 ppm for recommended chemicals.

Another contributing factor to the rate of asphaltene deposition is the composition of water in the wellbore. Salts contribute to the promotion of asphaltene deposition. Furthermore, the presence of Al^{3+} and Fe^{3+} ions in the water also causes an increase in the amount of deposition. For these reasons, although laboratory tests are helpful to identify suitable chemicals, the best method to determine the optimum concentration is field testing. It is also a good idea to test the chemicals over a period of time (a few days or more) to evaluate their performance and compare it with the incumbent chemical's performance. The best chemical is the one that minimizes the amount of asphaltene deposition at the lowest possible cost per unit barrel of crude. At higher water-cut fields use of a demulsifier that produces the fastest and cleanest separation of oil and water at the lowest possible cost per unit barrel of crude is recommended.

The water associated with oil sample A was separated and analyzed for metal elements that may affect the amount of asphaltene precipitation. The instrument used for the water analysis was the Sequential Wavelength Dispersive X-Ray Fluorescence Spectrometer or SWD XRF–ZSX available in the Chemical Engineering Laboratory which is capable of analyzing elements from Be to U with a microanalysis to analyze samples as small as 500 μm . The instrument is recommended for an elemental analysis of solids, liquids, powders, alloys, and thin films. The results are given in Table 9. The water weight is 81.18% and the remaining is total dissolved solid.

Table 9. Test results (in both ppm and wt.%) for water associated with oil sample A collected on 28 February 2021.

Comp.	Na	Mg	Al	Si	S	Cl	K	Ca	Br	Sr	Ba	W	H ₂ O
Unit	mass%	mass%	mass%	mass%	mass%	mass%	mass%	mass%	mass%	mass%	mass%	mass%	mass%
Result	5.205	0.243	0	0.001	0.019	11.42	0.241	1.530	0.082	0.062	0.021	0.001	81.18
Unit	ppm	ppm	Ppm	ppm	ppm	ppm	ppm	ppm	ppm	ppm	ppm	ppm	ppm
Result	52046	2432	<29	15	192	114169	2406	15291	822	618	214	11	52046

The water was also analyzed for Al³⁺ and Fe³⁺ ions by another instrument microwave plasma (Agilent model—4100 MP-AES) and the result indicated that the Al content was 0.4 ppm and the Fe content of the water was 3.29 ppmw. The total amount of dissolved solids (TDS), as determined by a simple evaporation and drying method (without the use of any instrument), was determined to be about 21 wt.%, which is just slightly above 19 wt.% determined by the XRF instrument given in the above table.

3.5. Calculation of the Required Amount of Inhibitor, Cost Analysis, and Final Recommendations

The volume rate of the inhibitor required to be injected for a certain oil production rate and ppm can be calculated from one of the following simple relations in gallon, liter, or kg:

$$\text{Required Inhibitor Rate, Gallon/day} = (4.2 \times 10^{-5}) \times (\text{Oil Rate, BPSD}) \times (\text{ppm});$$

$$\text{Required Inhibitor Rate, Liters/day} = (1.59 \times 10^{-4}) \times (\text{Oil Rate, BPSD}) \times (\text{ppm});$$

$$\text{Required Inhibitor Rate, Kg/day} = (1.431 \times 10^{-4}) \times (\text{Oil Rate, BPSD}) \times (\text{ppm});$$

where:

Required Inhibitor Rate, Gallon/d = Required Inhibitor Rate in Gallons per day;

Required Inhibitor Rate, Liter/d = Required Inhibitor Rate in Liters per day

ppm = Desired concentration of inhibitor in oil in ppm;

Required Inhibitor Rate, Kg/d = Required Inhibitor Rate in kilogram per day;

Oil Rate (BPSD) = Oil Production Rate (after separator and excluding water cut and associated gas) in BPSD (barrel per service day);

Unit Conversion Factors: 1 US Gallon = 3.785 liters, 1 barrel = 42 US Gallons, 1 ppm = 1 part per million = 1×10^{-6} v/v or g/g. Approximate density of the inhibitor ≈ 900 kg/m³ (0.9 g/mL).

For example, for each 1000 bbl of oil to have an inhibitor concentration of 300 ppm, a volume of 47.7 L (12.6 US Gallons) or about 43 kg of inhibitor should be injected into the wellbore. If the inhibitor price is taken at 5 EUR/kg, the chemical injection cost would be about 200 EUR for each 1000 bbl of crude oil produced. The above relations show that the inhibitor rate is directly proportional to the oil flow rate or desired concentration in oil in ppm.

Any selected chemical, when used over a period of time, must be economically attractive and contribute to the overall return on investment (ROI). Cost analysis can be gauged through ROI, which can be calculated as:

$$\text{ROI} = (\text{Incremental Revenue} - \text{Incremental Cost of Treatment}) / (\text{Incremental Cost of Treatment}) \times 100$$

where:

Incremental Revenue in USD = (oil production after treatment, BPSD – oil production before treatment, BPSD) \times (oil price, \$/bbl);

Incremental Cost of Treatment in USD = (Rate of inhibitor injected in Gallons per day) \times (unit price of inhibitor, \$/gallon);

It is very important that a chemical is injected at the right and optimized dose. An overdose or a low dosage may cause adverse effects resulting in an increased amount of

asphaltene deposition. One way to avoid this is a regular monitoring plan and testing in the field more often.

4. Discussion

The employed methods to determine the asphaltene stability of studied crude oil samples denoted that crude oil samples A and B are unstable (or mildly unstable) (Figures 8 and 9). Thus, one may expect that they would be prone to precipitate asphaltenes and form sediments in the process of crude oil production. In order to minimize the probability of asphaltene precipitation 11 commercial chemical additives designed to inhibit the sediment formation process were examined. It was found that six of these additives were capable of asphaltene precipitation minimization (Figure 14, Table 7). The IR-spectra (Figures S1–S7) of these six additives showed the presence of valence oscillations in the region $3000\text{--}2800\text{ cm}^{-1}$, typical for the presence of aliphatic groups, with bands at about 2960 and 2870 cm^{-1} corresponding to the symmetric and asymmetric oscillation of CH_3 groups, whilst those at 2860 cm^{-1} corresponding to the symmetric oscillation of CH_2 groups, with bands at around 1600 and 1500 cm^{-1} which are probably a result from the oscillation of C-C bonds in the aromatic ring. There is a maximum at around 1770 cm^{-1} which is an indicator of the presence of C=O ester and cyclic ester. The band at around 1700 cm^{-1} is probably a result of the oscillation of the C=O bond participating in the carboxylic group. There is a band at about 1460 cm^{-1} characterizing the asymmetric oscillation of CH_3 groups. Therefore, the additives A1–A6 could be considered to be composed of aliphatic, aromatic, and organic acid derivative components. However, the ratio between these components seems to be different for the distinct additives judging from the different areas of the peaks responsible for the diverse component structures.

The additives A9, A10, and A11 exhibit the same valence oscillations as those of additives A1–A6, however with different intensities (Figures S10–S12). This suggests a different ratio between the aliphatic, aromatic, and organic acid derivative components. The additives A9, A10, and A11 exhibited either a very small inhibiting effect or the promotion of asphaltene precipitation (Figure 15, Table 7). Therefore, the ratio between the component structures seems to be crucial for the performance of the chemical additive. Barsenas et al. [30] showed that the same inhibitor during the changing of the medium (from toluene at $50\text{ }^\circ\text{C}$ to *o*-dichlorobenzene at $90\text{ }^\circ\text{C}$) turned from an asphaltene inhibitor into an asphaltene aggregation promoter. Thus, the ratio between the aliphatic, aromatic, and organic acid derivative components seems to control the efficiency of the additive as an asphaltene precipitation inhibitor. The IR spectra of the additive A7 (Figure S8) showed that it contains bands in the region of $3000\text{--}2800\text{ cm}^{-1}$ at 1463 and 1380 cm^{-1} , which is typical for the presence of aliphatic groups. Three broad bands at about $2700\text{--}2500\text{ cm}^{-1}$, $2400\text{--}2100\text{ cm}^{-1}$, and $1800\text{--}1600\text{ cm}^{-1}$ are due to the presence of hydroxyl groups that are strongly involved in hydrogen bonding to phosphoryl oxygen atoms in acidic organophosphorus acids. The very strong and broad band at 1213 cm^{-1} is due to the P=O stretching vibration. The strongest and also very broad absorption at $\sim 1024\text{ cm}^{-1}$ is attributed to the P-O stretching vibrations. Several weak bands between $881\text{--}650\text{ cm}^{-1}$ are characteristic of the ethylhexyl groups. The absorption intensities at 1607 cm^{-1} and 1505 cm^{-1} correspond to carbon-carbon stretching vibrations in the aromatic ring, indicating the presence of aromatic compounds. Obviously, the existent ratio between the component structures in additive A7 is unfavorable for asphaltene precipitation in crude oil sample A, making it an asphaltene precipitation promoter instead of an inhibitor. This component structure ratio in A7, however, as evident from the data in Figure 15e (Table 8) which does not make it an asphaltene precipitation promoter when H-Oil ATB is treated, which confirms again that the additive performance is oil specific, as reported in another research [23]. A more informative view of the functional groups identified to be present in the 11 studied additives by the use of FTIR is presented in Table 10.

Table 10. Assignments of IR absorption bands in the spectra of all tested additives (A1–A11).

A1	A2	A3	A4	A5	A6	A7	A8	A9	A10	A11	Functional Group/ Assignments
Group Frequency, Wavenumbers (cm⁻¹)											
3450	3449	3483		3448	3447	3400	3426		3386		–OH; –NH stretch
						3002		3017			=C–H stretch
2963	2957	2963	2959	2956	2956	2961	2953	2964	2953	2958	C–H asymmetric stretch
2931	2926	2933	2926	2926	2927	2930	2925	2925	2925	2925	C–H asymmetric stretch
2873	2872	2872	2872	2871	2873	2873				2871	C–H symmetric stretch
	2856			2855	2858		2854	2855	2855	2856	C–H asymmetric stretch
1736	1770	1736	1735			1772		1780		1735	C=O stretch
							1717			1711	
	1706			1701	1702					1702	
1607	1608	1607	1607	1602	1602	1607		1607		1607	carbon-carbon stretching vibrations in the aromatic ring
								1516	1577		
1505	1506	1505	1505	1505	1505	1505		1505			
1462	1464	1461	1462	1464	1466	1463	1459	1455	1466	1462	C–H bend: CH ₂
1386/1366		1385/1366				1389/1366				1377/1366	CH(CH ₃) ₂
				1366		1380	1377	1377			C–H bend: CH ₃
	1388/1377/1366		1385/1377/1366							1389/1377/1366	C(CH ₃) ₃
						1213					P=O stretch
						1024					P–O stretch
900–700	900–700	900–700	900–700	900–700	900–700				900–700	900–700	C–H out-of-plane bend
							750–400				Metal–oxygen stretch

The data in Table 8 (Figure 15) displays that additives A2, A3, and A4 demonstrated good performance as asphaltene precipitation inhibitors also when H-Oil ATB was treated. The efficiency of the asphaltene precipitation reduction, however, was almost double as low as that of the crude oil sample A (Table 7) implying that the efficiency of asphaltene inhibition is also oil specific. The additive A5 being Nr.2 in the ranking of asphaltene inhibitors for crude oil sample A (Table 7) also showed precipitation reduction when H-Oil ATB sample 2 was treated (Figure 15d). However, with the H-Oil ATB, the ranking of A5 is number five indicating again that the efficiency of asphaltene inhibitor performance is oil specific. Therefore, the selection of a chemical additive to inhibit deposit formation during oil production or during refining operations is a subtle matter.

The proper selection can provide an opportunity to improve profitability by increasing the cycle length of the operation equipment, reducing maintenance costs, and creating higher reliability in crude oil production and oil refining facilities to overcome chemical costs. The improper selection, however, can have a deleterious effect on the economics of both crude oil production and refining.

5. Conclusions

Two crude oil samples (A, and B) from the same deep reservoir located in Kuwait were analyzed for asphaltene instability. A simulator was developed to construct asphaltene phase diagrams and to show regions of instability. The crude oil samples were qualified as unstable or mildly unstable based on the five methods applied to assess crude oil stability. Eleven commercial chemical inhibitors were examined to reduce asphaltene precipitation by the use of an asphaltene dispersion test. IR spectra of the inhibitors revealed that they were

composed of aliphatic, aromatic, and organic acid derivative components in different ratios. Six of the inhibitors were ranked as suitable for field application, reducing the asphaltene precipitation between 67 and 75%. The other five chemical additives were considered inappropriate since they either had no effect or promoted asphaltene precipitation.

Aside from crude oil sample two, H-Oil ATB samples were also tested with six commercial chemical inhibitors. It was found that four of the inhibitors reduced the asphaltene precipitation in the H-Oil ATBs as they did when the crude oil sample was treated. However, their efficiency was lower than that observed during the crude oil treatment. An inefficient additive for the crude oil sample was found efficient when the H-Oil ATBs were treated. An additive that promoted asphaltene precipitation during crude oil treatment did not show the same promoting effect when the H-Oil ATBs were treated. This confirms the conclusion made by other researchers that additive performance is oil specific. The paper concluded with some recommendations for the field application of chemical inhibitors.

Supplementary Materials: The following supporting information can be downloaded at: <https://www.mdpi.com/article/10.3390/pr11030818/s1>, Figure S1: IR-spectra of additive A1; Figure S2: IR-spectra of additive A2; Figure S3: IR-spectra of additive A3; Figure S4: IR-spectra of additive A4; Figure S5: IR-spectra of additive A5; Figure S6: IR-spectra of additive A6; Figure S7: Combined IR-spectra of the additives A1, A2, A3, A4, A5, and A6.; Figure S8: IR-spectra of additive A7; Figure S9: IR-spectra of additive A8; Figure S10: IR-spectra of additive A9; Figure S11: IR-spectra of additive A10; Figure S12: IR-spectra of additive A11; Figure S13: Combined IR-spectra of the additives A7, A8, A9, A10, and A11.

Author Contributions: Conceptualization, M.R.R. and A.Q.; Data curation; Formal analysis, J.F.P.; Funding acquisition, N.A.-K.; Investigation, D.S., I.S., R.N. and V.T.; Project administration, A.S.A.; Resources, N.A.-K. and J.F.P.; Software, M.R.R., A.S.A. and J.F.P.; Supervision, M.R.R.; Validation, A.Q., A.S.A. and N.A.-K.; Visualization, A.Q.; Writing—original draft, M.R.R. and D.S.; Writing—review & editing, M.R.R. and D.S. All authors have read and agreed to the published version of the manuscript.

Funding: Kuwait Oil Company.

Data Availability Statement: Not applicable.

Acknowledgments: Part of this manuscript was presented orally at the session: Advances in Petroleum Production and Processing at the 2022 AIChE Annual Meeting, 13–18 November 2022, Phoenix, AZ, USA. Funding received from KOC to conduct the work is greatly appreciated. The author Radoslava Nikolova acknowledges the support from Bulgarian Ministry of Education and Science under the National Program “Young Scientist and Postdoctoral Students-2”.

Conflicts of Interest: The authors declare no conflict of interest.

Nomenclature

ADEPT	Asphaltene Deposition Tool
ADs	Asphaltene Dispersants
ADT	Asphaltene Dispersant Test
AIs	Asphaltene Inhibitors
APD	Asphaltene Phase Diagrams
APDD	Asphaltene Phase Diagram and Deposition
API Gravity	The American Petroleum Institute gravity
ATB	H-Oil hydrocracked atmospheric residue
BHT	bottom hole temperature
BP	Bubble point
BPSD	Barrel Per Stream Day
CII	Colloidal Instability Index
CME	Constant Mass Experiment

cP	Centipoise
CPA-EOS	Cubic-plus-association equation of state
cSt	Centistokes
EOR	Enhanced Oil Recovery
GC	Gas chromatography
GOR, scf/bbl	Gas Oil Ratio, standard cubic feet of gas per barrel of oil
H-Oil ATB	H-Oil hydrocracked atmospheric residue
IBP	Initial Boiling Point, °C
ID	Identity
IR	Infrared
KOC	Kuwait Oil Company
Mol. Wt.	Molecular weight
MW ₇₊	Molecular weight of C ₇₊
PC-SAFT	Perturbed chain statistical associating fluid theory
Psia	Pounds per square inch absolute
Psig	Pounds per square in gauge
PVT	pressure–volume temperature
ROI	return on investment
SWD XRF–ZSX	Sequential Wavelength Dispersive X-ray Fluorescence Spectrometer
UAOP	Upper asphaltene onset pressure
VBA codes	Visual Basic for Applications
XRF	X-ray fluorescence

References

- Riazi, M.R. *Characterization and Properties of Petroleum Fractions*; ASTM International: Conshohocken, PA, USA, 2005.
- Mousavi-Dehghani, S.A.; Riazi, M.R.; Vafaie-Sefti, M.; Mansoori, G.A. An Analysis of methods for determination of onsets of asphaltene phase separations. *J. Pet. Sci. Eng.* **2004**, *42*, 145–156. [[CrossRef](#)]
- Riazi, M.R. *Characteristics of Asphaltenic and Waxy Oils*; Annual AIChE Meeting, Session on Heavy Oil and Flow Assurance: San Francisco, CA, USA, 2013.
- Akbarzadeh, K.; Dhillon, A.; Svrcek, W.Y.; Yarranton, H.W. Methodology for the characterization and modeling of asphaltene precipitation from heavy oils diluted with n-alkanes. *Energy Fuels* **2004**, *18*, 1434–1441. [[CrossRef](#)]
- Fakher, S.; Ahdaya, M.; Elturki, M.; Imqam, A. An experimental investigation of asphaltene stability in heavy crude oil during carbon dioxide injection. *J. Pet. Explor. Prod. Technol.* **2020**, *10*, 919–931. [[CrossRef](#)]
- Mohammed, I.; Mahmoud, M.; Al Shehri, D.; El-Husseiny, A.; Alade, O. Asphaltene precipitation and deposition: A critical review. *J. Pet. Sci. Eng.* **2021**, *2*, 107956. [[CrossRef](#)]
- Pereira, V.J.; Setaro, L.L.O.; Costa, G.M.N.; de Melo, S.A.B. Evaluation and improvement of screening methods applied to asphaltene precipitation. *Energy Fuels* **2016**, *31*, 3380–3391. [[CrossRef](#)]
- Yen, A.; Yin, Y.R.; Asomaning, S. *Evaluating Asphaltene Inhibitors: Laboratory Tests and Field Studies*; SPE International Symposium on Oilfield Chemistry: Houston, TX, USA, 2001; Paper Number: SPE-65376-MS. [[CrossRef](#)]
- Stankiewicz, A.B.; Flannery, M.D.; Fuex, N.A.; Broze, G.; Couch, J.L.; Dubey, S.T.; Iyer, S.D.; Ratulowski, J.; Westerich, J.T. Prediction of asphaltene deposition risk in E&P operations. In Proceedings of the 3rd International Symposium on Mechanisms and Mitigation of Fouling in Petroleum and Natural Gas Production, AIChE 2002 Spring National Meeting, New Orleans, LA, USA, 10–14 March 2002; paper 47C. pp. 410–416.
- De Boer, R.B.; Leelooyer, K.; Eigner, M.R.P.; van Bergen, A.R.D. 1995, Screening of crude oils for asphalt precipitation: Theory, practice, and the selection of inhibitors. *SPE Prod. Oper.* **1995**, *10*, 55–61. [[CrossRef](#)]
- Chapman, W.G.; Gubbins, K.E.; Jackson, G.; Radosz, M. SAFT: Equation of state solution model for associating fluids. *Fluid Ph. Equilibria* **1989**, *52*, 31–38. [[CrossRef](#)]
- Gross, J.; Sadowski, G. Perturbed chain SAFT: An equation of state on a perturbed theory for chain molecules. *Ind. Eng. Chem. Res.* **2001**, *40*, 1244–1260. [[CrossRef](#)]
- Kurup, A.S.; Wang, J.; Subramani, H.J.; Buckley, J.; Creek, J.L.; Chapman, W.G. Revisiting asphaltene deposition tool (ADEPT): Field application. *Energy Fuels* **2012**, *26*, 5702–5710. [[CrossRef](#)]
- Kurup, A.S.; Vargas, F.M.; Wang, J.; Buckley, J.; Creek, J.L.; Subramani, H.J.; Chapman, W.G. Development and application of an asphaltene deposition tool (ADEPT) for well bores. *Energy Fuels* **2011**, *25*, 4506–4516. [[CrossRef](#)]
- Gonzalez, D.L.; Ting, P.D.; Hirasaki, G.J.; Chapman, W.G. Prediction of asphaltene instability under gas injection with the PC-SAFT equation of state. *Energy Fuels* **2005**, *19*, 1230–1234. [[CrossRef](#)]
- Ting, P.D.; Gonzalez, D.L.; Hirasaki, G.J.; Chapman, W.G. *Application of the of PC-SAFT Equation of State to Asphaltene Phase Behavior, Asphaltene, Heavy Oils, and Petroleomics*; Springer: Berlin/Heidelberg, Germany, 2007; pp. 301–327.
- Panuganti, S.R.; Tavakkoli, M.; Vargas, F.M.; Gonzalez, D.L.; Chapman, W.G. SAFT Model for upstream asphaltene applications. *Fluid Ph. Equilibria* **2013**, *359*, 2–16. [[CrossRef](#)]

18. Nazari, F.; Asssareh, M. An effective asphaltene modeling approach using PC-SAFT with detailed description for gas injection conditions. *Fluid Phase Equilib.* **2021**, *532*, 112937. [[CrossRef](#)]
19. Kelland, M.A. *Production Chemicals for the Oil and Gas Industry*; Taylor & Francis, CRC Press: New York, NY, USA, 2009.
20. Da Silva, R.; Haraguchi, A.C.; Notrispe, L.; Loh, F.R.; Mohamed, W.R.S. Interfacial and colloidal behavior of asphaltenes obtained from Brazilian crude oils. *J. Pet. Sci. Eng.* **2001**, *32*, 201–216.
21. Ramdass, K.K.; Chakrabarti, D.P. Effectiveness of Biodiesel as an Alternative Solvent for the Remediation of Asphaltene Deposits. Available online: https://www.researchgate.net/publication/324128907_Effectiveness_of_Biodiesel_as_an_Alternative_Solvent_for_the_Remediation_of_Asphaltene_Deposits (accessed on 11 January 2023).
22. Mahdi, M.; Kharrat, R.; Hamoule, T. 2018, Screening of inhibitors for remediation of asphaltene deposits: Experimental and modeling study. *Petroleum* **2018**, *4*, 168–177.
23. Abrahamsen, E.L. Organic Flow Assurance: Asphaltene Dispersant/Inhibitor Formulation Development through Experimental Design. Ph.D. Thesis, University of Stavanger, Stavanger, Norway, 2012.
24. Stratiev, D.; Dinkov, R.; Shishkova, I.; Sharafutdinov, I.; Ivanova, N.; Mitkova, M.; Yordanov, D.; Rudnev, N.; Stanulov, K.; Artemiev, A.; et al. What is behind the high values of hot filtration test of the ebullated bed residue H-Oil hydrocracker residual oils? *Energy Fuels* **2016**, *30*, 7037–7054. [[CrossRef](#)]
25. Schermer, W.E.M.; Melein, P.M.J.; van den Berg, F.G.A. Simple techniques for evaluation of crude oil compatibility. *Pet Sci Technol.* **2004**, *22*, 7–8, 1045–1054. [[CrossRef](#)]
26. Stratiev, D.; Shishkova, I.; Tavlieva, M.; Kirilov, K.; Dinkov, R.; Yordanov, D.; Yankova, L.; Toteva, V.; Nikolova, R. Inhibiting sediment formation in an extra light crude oil and in a hydrocracked atmospheric residue by commercial chemical additives. *J. Chem. Technol. Metall.* **2022**, *57*, 63–75.
27. Melendez-Alvarez, A.A.; Garcia-Bermudes, M.; Tavakkoli, M.; Doherty, R.H.; Meng, S.; Abdallah, D.S.; Vargas, F.M. On the evaluation of the performance of asphaltene dispersants. *Fuel* **2016**, *179*, 210–220. [[CrossRef](#)]
28. Ghloum, E.F.; Al-Qahtani, M.; Al-Rashid, A. Effect of inhibitors on asphaltene precipitation for Marrat Kuwaiti reservoirs. *J. Petrol. Sci. Eng.* **2010**, *70*, 99–106. [[CrossRef](#)]
29. Jamaluddin, A.K.M.; Creek, J.; Kabir, C.S.; McFadden, J.D.; D’Cruz, D.; Manakalathil, J.; Joshi, N.; Ross, B. Laboratory techniques to measure thermodynamic asphaltene instability. *J. Can. Pet. Technol.* **2002**, *41*, 44–52. [[CrossRef](#)]
30. Barcenas, M.; Orea, P.; Buenrostro-González, E.; Zamudio-Rivera, L.S.; Duda, Y. Study of medium effect on asphaltene agglomeration inhibitor efficiency. *Energy Fuels* **2008**, *22*, 1917–1922. [[CrossRef](#)]
31. Kor, P.; Kharrat, R. 2016, Modeling of asphaltene particle deposition from turbulent oil flow in tubing: Model validation and a parametric study. *Petroleum* **2016**, *2*, 393–398. [[CrossRef](#)]
32. Amiri, R.; Khamsehchi, E.; Ghaffarzadeh, M.; Kardani, N. Static and dynamic evaluation of a novel solution path on asphaltene deposition and drag reduction in flowlines: An experimental study. *J. Pet. Sci. Eng.* **2021**, *205*, 108833. [[CrossRef](#)]
33. Nezhad, S.R.; Kiomarsiyan, A.; Darvish, H. A novel experimental study on inhibition of asphaltene deposition. *Pet Sci. Technol.* **2022**, 1–9. [[CrossRef](#)]
34. Ali, S.I.; Lalji, S.M.; Haneef, J.; Tariq, S.M.; Zaidi, S.F.; Anjum, M. Performance evaluation of asphaltene inhibitors using integrated method—ADT coupled with spot test. *Arab. J. Geosci.* **2022**, *15*, 674. [[CrossRef](#)]
35. Khormali, A.; Moghadasi, R.; Kazemzadeh, Y.; Struchkov, I. Development of a new chemical solvent package for increasing the asphaltene removal performance under static and dynamic conditions. *J. Pet. Sci. Eng.* **2021**, *206*, 109066. [[CrossRef](#)]

Disclaimer/Publisher’s Note: The statements, opinions and data contained in all publications are solely those of the individual author(s) and contributor(s) and not of MDPI and/or the editor(s). MDPI and/or the editor(s) disclaim responsibility for any injury to people or property resulting from any ideas, methods, instructions or products referred to in the content.